Chapter 5

Aircraft Landing Control Using the H-inf Control and the Dynamic Inversion Technique

Romulus Lungu and Mihai Lungu

Additional information is available at the end of the chapter

http://dx.doi.org/10.5772/62666

Abstract

The chapter presents the automatic control of aircraft during landing, taking into account the sensor errors and the wind shears. Both planes—longitudinal and lateral-directional—are treated; the new obtained automatic landing system (ALS) will consists of two subsystems—the first one controls aircraft motion in longitudinal plane, while the second one is for the control of aircraft motion in lateral-directional plane. These two systems can be treated separately, but in the same time, these can be put together to control all the parameters which interfere in the dynamics of aircraft landing. The two new ALSs are designed by using the H-inf control, the dynamic inversion, optimal observers, and reference models. To validate the new obtained ALS, one uses the dynamics associated to the landing of a Boeing 747, software implements the theoretical results and analyzes the accuracy of the results and the precision standards' achievement with respect to the requirements of the Federal Aviation Administration (FAA).

Keywords: Landing, H-inf control, Dynamic inversion, Observer, Reference model

1. Introduction

Landing is one of the most critical stages of flight; the aircraft has to perform a precise maneuver in the proximity of the ground to land safely at a suitable touch point with acceptable sink rate, speed, and attitude. During aircraft landing, the presence of different unknown or partially known disturbances in aircraft dynamics leads to the necessity of using modern automatic control systems. Sometimes, the conventional controllers are difficult to use due to the drastically changing of the atmospheric conditions and the dynamics of aircraft [1, 2]. In order to control aircraft landing, the feedback linearization has been used in [3], but the drawback of this method is that all the parametric plant uncertainties must appear in the same equation of the state-space representation. Other automatic landing systems (ALSs) use feed-forward neural networks based on the back propagation learning

algorithms [4]; the main disadvantage is that the neural networks require a priori training on normal and faulty operating data. From the optimal synthesis' point of view, a mixed technique for the H_2/H_∞ control of landing has been introduced by Shue and Agarwal [5], while Ochi and Kanai [6] have used the H-inf technique for the same purpose; the negative point of these papers is the robustness of the controllers since the sensor errors and other external disturbances are not considered. The fuzzy logic has been also used to imitate the pilot's experience in compromising between trajectory tracking and touchdown safety [7]. In other studies [8], it has been proved that an intelligent on-line-learning controller is helpful in assisting different baseline controllers in tolerating a stuck control surface in the presence of strong wind.

The main drawback of all the papers dealing with aircraft landing is that the designed ALSs are designed either for the longitudinal plane or for the lateral-directional plane. Our work focuses on aircraft automatic control in the two planes, during landing, by using the linearized dynamics of aircraft, the H-inf control, and the dynamic inversion concept, taking into consideration the wind shears, the crosswind, and the errors of the sensors. Our aim is to design a new landing control system (both planes) which cancels the negative effect of wind shears, the crosswind, and the errors of the sensors. According to this work's authors, little progress has been reported for the landing flight control systems (using the H-inf control and the dynamic inversion) handling all the above presented problems.

The three phases of a typical landing procedure are: the initial approach, the glide slope, and the flare [1, 9]. The initial approach involves a descend of the aircraft from the cruise altitude to approximately 420 m (heavy aircraft). Aircraft pitch, attitude, and speed must be controlled during the glide slope path; its speed should be constant during this stage of landing. For a Boeing 747, the pitch should be between −5 and 5 degrees, while the sink rate should be 3 m/s. For the same type of aircraft, when the altitude is 20–30 m above the ground, a flare maneuver should be accomplished and, therefore, the slope angle control system is disengaged; during the flare, aircraft pitch angle is adjusted (between 0 and 5 degrees) for a soft touchdown of the runway. These issues will be achieved by the first system presented in this chapter—the one for the control of aircraft trajectory in the longitudinal plane. The motion of aircraft in lateral plane should be done without errors, this meaning the cancel of aircraft deviation with respect to the runway direction; for this purpose, flight direction automatic control systems are necessary; this issue will be achieved by the second system presented in this chapter—the one for the control of aircraft trajectory in the lateral-directional plane.

2. Design the first subsystem of the ALS (longitudinal plane)

2.1. Aircraft dynamics in longitudinal plane

The linearized dynamics of aircraft in longitudinal plane is described by the state equation [10]: $\dot{\boldsymbol{x}}_{long} = A_{long}\boldsymbol{x}_{long} + B_{long}\boldsymbol{u}_{long} + G_{long}\tilde{\boldsymbol{u}}_{long}$, with $\boldsymbol{x}_{long} = [\,u \quad w \quad q \quad \theta \quad H\,]^T$ – the state vector, $\boldsymbol{u}_{long} = [\,\delta_e \quad \delta_T\,]^T$ – the command vector, while $\tilde{\boldsymbol{u}}_{\boldsymbol{long}} = [\,V_{vx} \quad V_{vz}\,]^T$ is the vector of

disturbances – V_{vx} and V_{vz} (the components of the wind velocity along the longitudinal and vertical axes of the aircraft [11]); in the above equations, u is the longitudinal velocity of aircraft, w − the vertical velocity, q − the pitch angular rate, θ − the pitch angle, H − aircraft altitude, while δ_e and δ_T are the elevator deflection and the engine command, respectively. Because the vertical velocity w is much smaller than u, one can consider the velocity in longitudinal plane to be $V = \sqrt{u^2 + w^2} \cong u$ [10]; thus, the nominal value of V is considered to be $V_0 \cong u(0) = u_0$. The equations of the actuators are $\dot{\delta}_e = -\frac{1}{T_e}\delta_e + \frac{1}{T_e}\delta_{ec}$, $\dot{\delta}_T = -\frac{1}{T_T}\delta_T + \frac{1}{T_t}\delta_{Tc}$; δ_{ec} and δ_{Tc} are the commands applied to elevator engine, respectively. Considering δ_e and δ_T as new states, $\boldsymbol{x}_{long}$ and $\boldsymbol{u}_{long}$ become $\boldsymbol{x}_{long} = [u \quad w \quad q \quad \theta \quad H \quad \delta_e \quad \delta_T]^T$, $\boldsymbol{u}_{long} = [\delta_{ec} \quad \delta_{Tc}]^T$, while the new matrices $A_{long} \in R^{7\times 7}$, $B_{long} \in R^{7\times 2}$, and $G_{long} \in R^{7\times 2}$ are [10]:

$$A_{long} = \begin{bmatrix} a_{11} & a_{12} & 0 & a_{14} & 0 & b_{11} & b_{12} \\ a_{21} & a_{22} & a_{23} & 0 & 0 & b_{21} & b_{22} \\ a_{31} & a_{32} & a_{33} & 0 & 0 & b_{31} & b_{32} \\ 0 & 0 & 1 & 0 & 0 & 0 & 0 \\ 0 & a_{52} & 0 & a_{54} & 0 & 0 & 0 \\ 0 & 0 & 0 & 0 & 0 & -1/T_e & 0 \\ 0 & 0 & 0 & 0 & 0 & 0 & -1/T_T \end{bmatrix}, \; B_{long} = \begin{bmatrix} 0 & 0 \\ 0 & 0 \\ 0 & 0 \\ 0 & 0 \\ 0 & 0 \\ 1/T_e & 0 \\ 0 & 1/T_T \end{bmatrix}, \; G_{long} = \begin{bmatrix} g_{11} & g_{12} \\ g_{21} & g_{22} \\ g_{31} & g_{32} \\ 0 & 0 \\ 0 & 0 \\ 0 & 0 \\ 0 & 0 \end{bmatrix}. \tag{1}$$

2.2. Wind shears' model

By using the velocities' spectrum and generator filters having as inputs white noises, one can define the vector $\tilde{\boldsymbol{u}}_{long}$ which corresponds to a stochastic process. In this work, the disturbances are considered to be the wind shears, the equations associated to them being [10, 11]: $V_{vx} = -V_{vx_0}\sin(\omega_0 t)$, $V_{vz} = -V_{vz_0}[1-\cos(\omega_0 t)]$, $\omega_0 = 2\pi/T_0$, where T_0 is the flight time period inside the wind shear, while V_{vx_0} and V_{vz_0} are the maximum absolute values of the wind velocities with respect to aircraft longitudinal and vertical axes, respectively.

In order to calculate the matrix G_{long}, one replaces $\tilde{\boldsymbol{u}}_{long} = 0$ in the aircraft dynamics and, after that, one replaces u with $(u - V_{vx})$ and w with $(w - V_{vz})$; the coefficients of the velocities V_{vx}, V_{vz} and, thus, the elements of the matrix G_{long} are obtained as follows: $g_{11} = -a_{11}$, $g_{12} = -a_{12}$, $g_{21} = -a_{21}$, $g_{22} = -a_{22}$, $g_{31} = -a_{31}$, $g_{32} = -a_{32}$.

2.3. The general form of the control law (longitudinal plane)

One considers the vector $\boldsymbol{z}_{long} = [H \quad u]^T = C'_{long}\boldsymbol{x}_{long}$ that contains the system-controllable output variables, while the vector $\overline{\boldsymbol{z}}_{long} = \left[\overline{H} \quad \overline{u}\right]^T$ contains the reference variables (the imposed values of the flight altitude and velocity). The system output vector is $\boldsymbol{y}_{long}$, chosen of the following form: $\boldsymbol{y}_{long} = [H \quad \dot{H} \quad u \quad \dot{u} \quad \theta \quad q]^T = C_{long}\boldsymbol{x}_{long}$. Taking into account the differential equations of the states H and u, obtained from aircraft dynamics, by using $\boldsymbol{x}_{long}$ and $\boldsymbol{u}_{long}$ the matrices $A_{long}, B_{long}, G_{long}$, one yields:

$$C'_{long} = \begin{bmatrix} 0 & 1 \\ 0 & 0 \\ 0 & 0 \\ 0 & 0 \\ 1 & 0 \\ 0 & 0 \\ 0 & 0 \end{bmatrix}^T, \quad C_{long} = \begin{bmatrix} 0 & 0 & 0 & 0 & 1 & 0 & 0 \\ 0 & a_{52} & 0 & a_{54} & 0 & 0 & 0 \\ 1 & 0 & 0 & 0 & 0 & 0 & 0 \\ a_{11} & a_{12} & 0 & a_{14} & 0 & b_{11} & b_{12} \\ 0 & 0 & 0 & 1 & 0 & 0 & 0 \\ 0 & 0 & 1 & 0 & 0 & 0 & 0 \end{bmatrix}. \tag{2}$$

Now, by using $\overline{z}_{long}$ and the dynamic inversion principle, $\overline{x}_{long}$ and $\bar{u}_{long}$ are calculated with respect to $\overline{z}_{long}$ and, after that, the vector $\overline{y}_{long}$ is obtained by means of the equations [11]: $\dot{\overline{x}}_{long} = A_{long}\overline{x}_{long} + B_{long}\overline{u}_{long}$, $\overline{z}_{long} = C'_{long}\overline{x}_{long}$, $\overline{y}_{long} = C_{long}\overline{x}_{long}$. The command law is calculated with the formula [10]:

$$u_{long} = \overline{u}_{long} + u_{\infty long}, \tag{3}$$

where $u_{\infty long}$ is the optimal command that is calculated by means of the H-inf method [12, 13], while the component $\bar{u}_{long}$ is calculated by using the dynamic inversion.

2.4. Design of the control law's first component (longitudinal plane)

A coordinates' change is achieved by means of the transformation matrix $T \in R^{7 \times 7}$ [11]:

$$\begin{bmatrix} \xi \\ \eta \end{bmatrix} = Tx_{long}, \quad x_{long} = T^{-1}\begin{bmatrix} \xi \\ \eta \end{bmatrix}, \tag{4}$$

where ξ is a state vector consisting of the controlled variables and their derivatives, i.e. [11]: $\xi = [\, z_1 \quad \dot{z}_1 \quad \cdots \quad z_1^{(r_1-1)} \quad z_2 \quad \dot{z}_2 \quad \cdots \quad z_2^{(r_2-1)} \quad \cdots \quad z_p \quad \dot{z}_p \quad \cdots \quad z_p^{(r_p-1)} \,]^T$, with $z_i^{(r_i-1)}$– the $(r_i - 1)$ order derivatives of z_i; for the aircraft dynamics in longitudinal plane, $z_1 = H$, $z_2 = z_p = u$. The state vector η consists of all the state variables not included in the vector ξ; considering n to be the dimension of the square matrix T, one can easily deduce the dimension of the vector η as $n - r = n - \sum_{i=1}^{p} r_i$, where the values of the relative degrees r_i, $i = \overline{1,\ 2}$, are to be deduced later.

For the obtaining of the relative degrees r_1 and r_2, the equations of $\dot{u}$ and $\dot{w}$ are differentiated until terms containing the two components of the control law (δ_{ec}, δ_{Tc}) appears in the expressions of the variables $\ddot{u}$ and $\ddot{w}$; by time derivation of the variables $\ddot{u}$ and $\ddot{w}$ (expressed by using aircraft dynamics), it results some terms containing the variables $.\delta_{ec}$ and $.\delta_{Tc}$; these can be expressed by means of equations $\dot{\delta}_e = -\frac{1}{T_e}\delta_e + \frac{1}{T_e}\delta_{ec}$, $\dot{\delta}_T = -\frac{1}{T_T}\delta_T + \frac{1}{T_T}\delta_{Tc}$; one obtains $\ddot{u}$ and $\ddot{w}$ as functions of δ_{ec}, δ_{Tc}, and other states. Thus, the relative degree of the state u is $r_2 = 2$. In order to obtain the relative degree of the altitude (H), one derivates the differential equation associated to H, i.e. $\dot{H} = a_{52}w + a_{54}\theta$, and obtains $\ddot{H} = a_{52}\dot{w} + a_{54}\dot{\theta}$. is obtained. Therefore, the relative degree of the altitude is $r_1 = 3$. The following equations result:

http://dx.doi.org/10.5772/62666

$$\begin{aligned}\ddot{u} &= a_{11}^{'}u + a_{12}^{'}w + a_{13}^{'}q + a_{14}^{'}\theta + a_{16}^{'}\delta_e + a_{17}^{'}\delta_T + \frac{b_{11}}{T_e}\delta_{ec} + \frac{b_{12}}{T_T}\delta_{Tc} + g_{11}^{'}V_{vx} + g_{12}^{'}V_{vz} \\ &\quad + g_{11}\dot{V}_{vx} + g_{12}\dot{V}_{vz}, \\ \ddot{H} &= a_{51}^{'}u + a_{52}^{'}w + a_{53}^{'}q + a_{54}^{'}\theta + a_{56}^{'}\delta_e + a_{57}^{'}\delta_T + \frac{a_{52}b_{21}}{T_e}\delta_{ec} + \frac{a_{52}b_{22}}{T_T}\delta_{Tc} + g_{51}^{'}V_{vx} + g_{52}^{'}V_{vz} \\ &\quad + g_{51}^{''}\dot{V}_{vx} + g_{52}^{''}\dot{V}_{vz},\end{aligned} \tag{5}$$

with $a_{11}^{'} = a_{11}^2 + a_{12}a_{21}$, $a_{12}^{'} = a_{11}a_{12} + a_{12}a_{22}$, $a_{13}^{'} = a_{12}a_{23} + a_{14}$, $a_{14}^{'} = a_{11}a_{14}$, $a_{16}^{'} = a_{11}b_{11} + a_{12}b_{21} - \frac{b_{11}}{T_e}$, $a_{17}^{'} = a_{11}b_{12} + a_{12}b_{21} - \frac{b_{12}}{T_T}$, $g_{11}^{'} = a_{11}g_{11} + a_{12}g_{21}$, $g_{12}^{'} = a_{11}g_{12} + a_{12}g_{22}$, $a_{51}^{'} = a_{54}a_{31} + a_{52}(a_{21}a_{11} + a_{21}a_{12} + a_{23}a_{31})$, $a_{52}^{'} = a_{54}a_{32} + a_{52}\left(a_{21}a_{12} + a_{22}^2 + a_{23}a_{32}\right)$, $a^{53'} = a_{54}a_{33}$, $a_{54}^{'} = a_{52}(a_{22}a_{23} + a_{22}a_{33} + a_{21}a_{14})$, $a_{56}^{'} = a_{54}b_{31} + a_{52}\left(a_{21}b_{11} + a_{22}b_{21} + a_{23}b_{31} - \frac{1}{T_e}b_{21}\right)$, $a_{57}^{'} = a_{54}b_{32} + a_{52}\left(a_{21}b_{12} + a_{22}b_{22} + a_{23}b_{32} - \frac{1}{T_T}b_{22}\right)$, $g_{51}^{'} = a_{54}g_{31} + a_{52}\left(a_{21}g_{11} + a_{22}g_{21} + a_{23}g_{31}\right)$, $g_{52}^{'} = a_{54}g_{32} + a_{52}\left(a_{21}g_{12} + a_{22}g_{22} + a_{23}g_{33}\right)$, $g_{51}^{''} = a_{52}g_{21}$, $g_{52}^{''} = a_{52}g_{22}$.

Thus, the state vectors ξ and η are $\xi = [H \quad \dot{H} \quad \ddot{H} \quad u \quad \dot{u}]^T$, $\eta = [\theta \quad q]^T$. By means of the coordinates' change (4), considering $\tilde{\boldsymbol{u}}_{long} = 0$ and $\boldsymbol{u}_{long} = \bar{\boldsymbol{u}}_{long}$, aircraft dynamics gets the form [11]: $\begin{bmatrix}\dot{\xi}\\ \dot{\eta}\end{bmatrix} = \hat{A}_{long}\begin{bmatrix}\xi\\ \eta\end{bmatrix} + \hat{B}_{long}\,\overline{\boldsymbol{u}}_{long}$; $\hat{A}_{long} = TA_{long}T^{-1}$, $\hat{B}_{long} = TB_{long}$. If the matrices $\hat{A}_{long}$ and $\widehat{B}_{long}$ are partitioned with respect to the dimensions of the vectors ξ and η, it results [4]: $\begin{bmatrix}\dot{\xi}\\ \dot{\eta}\end{bmatrix} = \begin{bmatrix}\hat{A}_{long_{11}} & \hat{A}_{long_{12}}\\ \hat{A}_{long_{21}} & \hat{A}_{long_{22}}\end{bmatrix}\begin{bmatrix}\xi\\ \eta\end{bmatrix} + \begin{bmatrix}\hat{B}_{long_1}\\ \hat{B}_{long_2}\end{bmatrix}\overline{u}_{long}$. Imposing $\xi = \overline{\xi}$, $\dot{\xi} = \dot{\overline{\xi}}$, with $\overline{\xi} = [\overline{H} \quad \overline{\dot{H}} \quad \overline{\ddot{H}} \quad \overline{u} \quad \overline{\dot{u}}]^T$, $\dot{\overline{\xi}} = [\overline{\dot{H}} \quad \overline{\ddot{H}} \quad \overline{\dddot{H}} \quad \overline{\dot{u}} \quad \overline{\ddot{u}}]^T$, the vector $\bar{\boldsymbol{u}}_{long}$ is obtained as: $\overline{\boldsymbol{u}}_{long} = \widehat{B}_{long_1}^{+}\left(\dot{\overline{\xi}} - \widehat{A}_{long_{11}}\overline{\xi} - \widehat{A}_{long_{12}}\eta\right)$, with $\widehat{B}_{long_1}^{+}$ – pseudo-inverse of the matrix $\widehat{B}_{long_1}$.

For the obtaining of the matrix T, the vectors ξ and are replaced in (4) and the following differential equations result: $\dot{H} = a_{52}u + a_{54}\theta$, $\ddot{H} = a_{52}\dot{w} + a_{54}\dot{\theta}$, $\dot{\theta} = q$, $\dot{u} = a_{11}u + a_{12}w + a_{14}\theta + b_{11}\delta_e + b_{12}\delta_T$, $\dot{w} = a_{21}u + a_{22}w + a_{23}q + b_{21}\delta_e + b_{22}\delta_T$; one yields:

$$\begin{bmatrix}H\\ \dot{H}\\ \ddot{H}\\ u\\ \dot{u}\\ \theta\\ q\end{bmatrix} = \underbrace{\begin{bmatrix}0 & 0 & 0 & 0 & 1 & 0 & 0\\ 0 & a_{52} & 0 & a_{54} & 0 & 0 & 0\\ a_{52}a_{21} & a_{52}a_{22} & (a_{54} + a_{52}a_{23}) & 0 & 0 & a_{52}b_{21} & a_{52}b_{22}\\ 1 & 0 & 0 & 0 & 0 & 0 & 0\\ a_{11} & a_{12} & 0 & a_{14} & 0 & b_{11} & b_{12}\\ 0 & 0 & 0 & 1 & 0 & 0 & 0\\ 0 & 0 & 1 & 0 & 0 & 0 & 0\end{bmatrix}}_{T}\begin{bmatrix}u\\ w\\ q\\ \theta\\ H\\ \delta_e\\ \delta_T\end{bmatrix}. \tag{6}$$

Replacing the vectors $\overline{\xi} = [\overline{H} \quad \overline{\dot{H}} \quad \overline{\ddot{H}} \quad \overline{u} \quad \overline{\dot{u}}]^T$ and $\dot{\overline{\xi}} = [\overline{\dot{H}} \quad \overline{\ddot{H}} \quad \overline{\dddot{H}} \quad \overline{\dot{u}} \quad \overline{\ddot{u}}]^T$ into equation $\overline{\boldsymbol{u}}_{long} = \widehat{B}_{long_1}^{+}\left(\dot{\overline{\xi}} - \widehat{A}_{long_{11}}\overline{\xi} - \widehat{A}_{long_{12}}\eta\right)$, one obtains

$$\overline{\boldsymbol{u}}_{long} = \widehat{B}^{+}_{long_1}\left\{\begin{bmatrix} 0 & 0 & \overline{\overline{H}} & 0 & \overline{\overline{u}} \end{bmatrix}^T - \widehat{A}'_{long_{11}}\,\overline{\xi} - \widehat{A}_{long_{12}}\eta\right\}, \tag{7}$$

where $\widehat{A}'_{long_{11}}$ is calculated from $\widehat{A}_{long_{11}}$ making the substitutions: $\widehat{a}'_{12} = \widehat{a}_{12} - 1$, $\widehat{a}'_{23} = \widehat{a}_{23} - 1$, $\widehat{a}'_{45} = \widehat{a}_{45} - 1$, the other elements of the matrices $\widehat{A}_{long_{11}}$ and $\widehat{A}'_{long_{11}}$ being the same; $\widehat{a}_{ij}$, $i, j = \overline{1, 5}$ are the elements of the matrix $\widehat{A}_{long_{11}}$.

Replacing (7) in $\dot{\eta} = \widehat{A}_{long_{21}}\xi + \widehat{A}_{long_{22}}\eta + \widehat{B}_{long_2}\overline{\boldsymbol{u}}_{long}$, with $\xi = \overline{\xi}$, one obtains:

$$\dot{\eta} = \widehat{A}_{\eta}\eta + \widehat{B}_{y}\overline{\boldsymbol{Z}}, \tag{8}$$

where $\widehat{A}_{\eta} = \widehat{A}_{long_{22}} - \widehat{B}_{long_2}\widehat{B}^{+}_{long_1}\widehat{A}_{long_{12}}$, $\widehat{A}_{\xi} = \widehat{A}_{long_{21}} - \widehat{B}_{long_2}\widehat{B}^{+}_{long_1}\widehat{A}'_{long_{11}}$, $\widehat{B}_z\overline{\boldsymbol{z}}^{(r)}_{long} = \widehat{B}_{long_2}\widehat{B}^{+}_{long_1}\begin{bmatrix} 0 & 0 & \overline{\overline{H}} & 0 & \overline{\overline{u}} \end{bmatrix}^T$, $\overline{z}^{(r)}_{long} = [\,\overline{z}_1^{(r_1)} \quad \overline{z}_2^{(r_2)}\,]^T = [\,\overline{\overline{H}} \quad \overline{\overline{u}}\,]^T$, $\hat{B}_y = [\,\hat{B}_z \quad \hat{A}_{\xi}\,]$, $\overline{\boldsymbol{Z}} = [\,\overline{\boldsymbol{z}}^{(r)}_{long}\ \overline{\xi}\,]^T = [\,\overline{\overline{H}}\ \ \overline{\overline{u}}\ \ \overline{H}\ \ \overline{\dot{H}}\ \ \overline{\ddot{H}}\ \ \overline{u}\ \ \overline{\dot{u}}\,]^T$. If one considers $\hat{B}_{long_2}\,\hat{B}^{+}_{long_1} = \begin{bmatrix} \hat{b}_{11} & \hat{b}_{12} & \hat{b}_{13} & \hat{b}_{14} & \hat{b}_{15} \\ \hat{b}_{21} & \hat{b}_{22} & \hat{b}_{23} & \hat{b}_{24} & \hat{b}_{25} \end{bmatrix}$ then $\widehat{B}_z = \begin{bmatrix} \hat{b}_{13} & \hat{b}_{15} \\ \hat{b}_{22} & \hat{b}_{25} \end{bmatrix}$ Thus, for the calculation of the command vector $\bar{\boldsymbol{u}}_{long}$, one solves equation (8) and obtains the vector η and then uses the equation (7). From the expression of $\widehat{B}_z\overline{\boldsymbol{z}}^{(r)}_{long}$, it results: $\hat{B}^{+}_{long_1}[0\ \ 0\ \ \overline{\overline{H}}\ \ 0\ \ \overline{\overline{u}}\,]^T = \hat{B}^{+}_{long_2}\hat{B}_z\overline{\boldsymbol{z}}^{(r)}_{long}$, which, replaced in (7), leads to

$$\overline{\boldsymbol{u}}_{long} = \widehat{B}_u^{-1}\left(\overline{\boldsymbol{z}}^{(r)}_{long} - \widehat{B}_{\xi}\overline{\xi} - \widehat{B}_{\eta}\eta\right), \tag{9}$$

with $\widehat{B}_u^{-1} = \widehat{B}^{+}_{long_2}\widehat{B}_z$, $\widehat{B}_{\xi} = \widehat{B}_u\widehat{B}^{+}_{long_1}\widehat{A}'_{long_{11}}$, $\widehat{B}_{\eta} = \widehat{B}_u\widehat{B}^{+}_{long_1}\widehat{A}_{long_{12}}$. Therefore, $\bar{\boldsymbol{u}}_{long}$ can be obtained by means of equation (7) or by using equation (9).

2.5. Design of the control law's second component (longitudinal plane)

To calculate the second component of the control law $\boldsymbol{u}_{long}$, one combines the aircraft dynamics, the equations associated to $z_1 = H$ and $z_2 = u$, as well as the equation of the output vector $\boldsymbol{y}_{long}$:

$$\begin{bmatrix} \dot{\boldsymbol{x}}_{long} \\ z_1 \\ z_2 \\ \boldsymbol{y}_{long} \end{bmatrix} = \begin{bmatrix} A_{long} & B_{long} & G_{long} & 0_{(7\times 6)} \\ C_{0long} & D_{01long} & 0_{(1\times 2)} & 0_{(1\times 6)} \\ C_{1long} & D_{11long} & 0_{(1\times 2)} & 0_{(1\times 6)} \\ C_{long} & 0_{(6\times 2)} & 0_{(6\times 2)} & D_{22long} \end{bmatrix} \begin{bmatrix} \boldsymbol{x}_{long} \\ \boldsymbol{u}_{long} \\ \tilde{\boldsymbol{u}}_{long} \\ \boldsymbol{e}_{long} \end{bmatrix}, \tag{10}$$

with $C_{0long} = [\,0\ \ 0\ \ 0\ \ 0\ \ 1\ \ 0\ \ 0\,]$, $C_{1long} = [\,1\ \ 0\ \ 0\ \ 0\ \ 0\ \ 0\ \ 0\,]$, $D_{01long} = [\,c_1\ \ 0\,]$, $D_{11long} = [\,c_2\ \ 0\,]$, the matrix C_{long} has the form (2), while $D_{22long} = I_6$ for the vector containing

the sensor errors: $\boldsymbol{e}_{long} = [\, e_H \quad e_{\dot{H}} \quad e_u \quad e_{\dot{u}} \quad e_\Theta \quad e_q \,]^T$. The optimal control law has the form [10, 14]: $u_{\infty long} = -K_{\infty long}(\widehat{x}_{long} - \overline{x}_{long})$, $K_{\infty long} = {R_1}^{-1} {B_{long}}^T P_\infty$, $R_1 = D_{11long}^T D_{11long}$; $\boldsymbol{u}_{\infty long}$ minimizes the cost functional: $J_{long} = \frac{1}{2}\int_0^\infty z_2^T z_2 \mathrm{d}t = \frac{1}{2}\int_0^\infty [\boldsymbol{x}_{long}^T \underbrace{(C_{1\,long}^T C_{1\,long})}_{Q_1} \boldsymbol{x}_{long} + \boldsymbol{u}_{\infty\,long}^T \underbrace{(D_{11\,long}^T D_{11\,long})}_{R_1} \boldsymbol{u}_{\infty\,long}]\, \mathrm{d}t$.

The symmetric and positive defined matrix P_∞ is the stabilizing solution of the Riccati equation [15]:

$$A_{long}^T P_\infty + P_\infty A_{long} - P_\infty \left(B_{long} R_1^{-1} B_{long}^T - \mu_1^{-2} G_{long} G_{long}^T \right) P_\infty + Q_1 = 0. \tag{11}$$

Q_1 and R_1 are positive defined matrices, while μ_1 is a small enough positive scalar such that the Riccati equation (11) has a stabilizing solution [10]. To solve the H-inf control problem means to calculate the controller gain matrix ($K_{\infty\ long}$); the system has control inputs as well as disturbances; the control input ($\boldsymbol{u}_{long}$) is the controller's output, this becoming the actuators' input. The disturbances of the system ($\tilde{\boldsymbol{u}}_{long}$ and $\boldsymbol{e}_{long}$) are the exogenous inputs [10, 12, 13]. The H-inf control problem means to find a controller for the generalized plant such that the infinity norm of the transfer function relating exogenous inputs to performance outputs is minimum. The controller gain matrix ($K_{\infty\ long}$) has the general form $K_{\infty long} = R_1^{-1} B_{long}^T P_\infty$ [10, 12, 13], the optimal control law $\boldsymbol{u}_{\infty\,long}$ depending on $\Delta\widehat{\boldsymbol{x}}_{long} = \widehat{\boldsymbol{x}}_{long} - \overline{\boldsymbol{x}}_{long}$; to estimate this signal and the state $\widehat{\boldsymbol{x}}_{long}$, one borrowed the observer presented in [14], i.e.: $\Delta\dot{\widehat{\boldsymbol{x}}}_{long} = A_{long}\Delta\widehat{\boldsymbol{x}}_{long} + B_{long}\boldsymbol{u}_{long} + {} + G_{long}\tilde{\boldsymbol{u}}_{long} + L_{\infty long}\left(\Delta\boldsymbol{y}_{long} - C_{long}\Delta\widehat{\boldsymbol{x}}_{long}\right)$. The observer gain matrix $L_{\infty long}$ is calculated with the formula: $L_{\infty long} = P_\infty^* C_{long}^T \left(D_{22long}^T D_{22long} \right)^{-1}$, with P_∞^*– the stabilizing solution of the Riccati equation [15]:

$$A_{long} P_\infty^* + P_\infty^* A_{long}^T - P_\infty^* \left(C_{long}^T C_{long} - \mu_2^{-2} Q_1 \right) P_\infty^* + G_{long} G_{long}^T = 0; \tag{12}$$

μ_2 is a small positive scalar for which the Riccati equation (12) has a stabilizing solution.

3. Design the second subsystem of the ALS (lateral-directional plane)

3.1. Aircraft dynamics in lateral-directional plane

Before the start of the landing, two main stages in longitudinal plane (glide slope and flare), the pilot must cancel the aircraft lateral deviation with respect to the runway. This can be achieved by means of the second subsystem of the ALS designed in this chapter or by using other control systems for the flight direction control with radio navigation subsystem and equipment for the measurement of the distance between the aircraft and the radio markers. The linear model of the aircraft motion, in lateral-directional plane, can be described again by the state equation: $\dot{\boldsymbol{x}}_{lat} = A_{lat}\boldsymbol{x}_{lat} + B_{lat}\boldsymbol{u}_{lat} + G_{lat}\tilde{\boldsymbol{u}}_{lat}$, where $\boldsymbol{x}_{lat} = [\beta \;\; p \;\; r \;\; \varphi \;\; \psi \;\; Y \;\; \delta_a \;\; \delta_r]^T$, $\boldsymbol{u}_{lat} = [\, \delta_{a_c} \quad \delta_{r_c} \,]^T$, $\tilde{\boldsymbol{u}}_{lat} = V_{vy}$, with β – aircraft sideslip angle, φ and ψ are the roll angle and the

yaw angle, respectively, p − aircraft roll angular rate, r − the aircraft yaw angular rate, Y − aircraft lateral error, δ_a and δ_r − the ailerons and rudder's deflection angles, δ_{a_c} and δ_{r_c} − the roll and yaw commands (commands applied to the actuators), V_{vy} − the wind component having as direction—the aircraft the lateral axis, T_a and T_r − the effectors' time delay constants of the ailerons and rudder, respectively. The matrices A_{lat}, B_{lat}, and G_{lat} are [1]:

$$A_{lat} = \begin{bmatrix} a_{11} & a_{12} & a_{13} & a_{14} & 0 & 0 & b_{11} & b_{12} \\ a_{21} & a_{22} & a_{23} & 0 & 0 & 0 & b_{21} & b_{22} \\ a_{31} & a_{32} & a_{33} & 0 & 0 & 0 & b_{31} & b_{32} \\ 0 & 1 & 0 & 0 & 0 & 0 & 0 & 0 \\ 0 & 0 & 1 & 0 & 0 & 0 & 0 & 0 \\ -V_0 & 0 & 0 & 0 & V_0 & 0 & 0 & 0 \\ 0 & 0 & 0 & 0 & 0 & 0 & -\frac{1}{T_a} & 0 \\ 0 & 0 & 0 & 0 & 0 & 0 & 0 & -\frac{1}{T_r} \end{bmatrix}, \; B_{lat} = \begin{bmatrix} 0 & 0 \\ 0 & 0 \\ 0 & 0 \\ 0 & 0 \\ 0 & 0 \\ 0 & 0 \\ \frac{1}{T_a} & 0 \\ 0 & \frac{1}{T_r} \end{bmatrix}, \; G_{lat} = \begin{bmatrix} \frac{a_{11}}{V_0} \\ \frac{a_{21}}{V_0} \\ \frac{a_{31}}{V_0} \\ 0 \\ 0 \\ 1 \\ 0 \\ 0 \end{bmatrix}; \quad (13)$$

For the design of the second optimal subsystem of the ALS, let us consider the vector $\boldsymbol{z}_{lat} = [\, Y \quad \beta \,]^T = C'_{lat}\boldsymbol{x}_{lat}$—the vector of the system's controllable output variables and the vector $\overline{\boldsymbol{z}}_{lat} = \left[\, \overline{Y} \quad \overline{\beta} \,\right]^T$—the reference variables' vector, i.e. the desired values for the lateral deviation and the sideslip angle of the aircraft. The system's output vector is $\boldsymbol{y}_{lat} = [\, Y \quad \dot{Y} \quad \beta \quad \varphi \quad p \quad \psi \quad r \,]^T = C_{lat}\boldsymbol{x}_{lat}$; sensors' errors have been not taken into account here; knowing the forms of $\boldsymbol{z}_{lat}$ and $\boldsymbol{y}_{lat}$, the matrices C_{lat} and C'_{lat} can be easily deduced.

3.2. The general form of the control law (lateral-directional plane)

The command law is similar to the one for longitudinal plane; it is calculated with the formula:

$$\boldsymbol{u}_{lat} = \overline{\boldsymbol{u}}_{lat} + \boldsymbol{u}_{\infty lat}, \quad (14)$$

where $\boldsymbol{u}_{\infty lat}$ is the optimal command calculated by means of the H-inf method, while the component $\bar{\boldsymbol{u}}_{lat}$ is calculated by using the dynamic inversion [3, 12, 13]. For the design of the signal $\bar{\boldsymbol{u}}_{lat}$ there are used the dynamic inversion principle and the vectors $\overline{\boldsymbol{z}}_{lat} = C'_{lat}\overline{\boldsymbol{x}}_{lat}$, $\overline{\boldsymbol{y}}_{lat} = C_{lat}\overline{\boldsymbol{x}}_{lat}$, where $\overline{\boldsymbol{x}}_{lat}$ is determined from the equation $\dot{\overline{\boldsymbol{x}}}_{lat} = A\overline{\boldsymbol{x}}_{lat} + B_{lat}\overline{\boldsymbol{u}}_{lat}$.

3.3. Design of the control law's first component (lateral-directional plane)

First, one obtains the relative degrees of the variables $z_1 = Y$ and $z_2 = \beta$; these relative degrees are denoted here with r_1 and r_2, respectively. One derivates with respect to time the equations associated to Y and β (r_1 times and r_2 times, respectively) until the components of the command vector $\boldsymbol{u}_{lat}$, i.e. δ_{a_c} and δ_{r_c}, are obtained; the following equations have resulted:

$$\dddot{Y} = a'_{61}\beta + a'_{62}p + a'_{63}r + a'_{64}\varphi + a'_{67}\delta_a + a'_{68}\delta_r - \frac{V_0 b_{11}}{T_a}\delta_{a_c} - \frac{V_0 b_{12}}{T_r}\delta_{r_c} + \left(a_{31} - a'_{11}\right)V_{vy} - a_{11}\widetilde{V}_{vy},$$
$$\ddot{\beta} = a'_{11}\beta + a'_{12}p + a'_{13}r + a'_{14}\varphi + a'_{17}\delta_a + a'_{18}\delta_r + \frac{b_{11}}{T_a}\delta_{a_c} + \frac{b_{12}}{T_r}\delta_{r_c} + \frac{a'_{11}}{V_0}V_{vy} + \frac{a_{11}}{V_0}\widetilde{V}_{vy}, \tag{15}$$

where $a'_{11} = a_{11}^2 + a_{12}a_{21} + a_{13}a_{31}$, $a'_{12} = a_{11}a_{12} + a_{12}a_{22} + a_{13}a_{32} + a_{14}$, $a'_{13} = a_{11}a_{13} + a_{12}a_{23} + a_{13}a_{33}$, $a'_{14} = a_{11}a_{14}$, $a'_{17} = a_{11}b_{11} + a_{12}b_{21} + a_{13}b_{31} - b_{11}/T_a$, $a'_{18} = a_{11}b_{12} + a_{12}b_{22} + a_{13}b_{32} - b_{12}/T_r$, $a'_{61} = V_0\,(a_{31} - a'_{11})$, $a'_{62} = V_0\,(a_{32} - a'_{12})$, $a'_{63} = V_0\,(a_{33} - a'_{13})$, $a'_{64} = -V_0 a'_{14}$, $a'_{67} = V_0\,(b_{31} - a'_{17})$, $a'_{68} = V_0\,(b_{32} - a'_{18})$, $a'_{31} = a_{31} - a'_{11}$.

Thus, according to equations (15), the relative degrees are $r_1 = 3$ and $r_2 = 2$. The equations (15) may be combined in the equation of the vector $\boldsymbol{z}_{lat}^{(r)} = [\,\dddot{Y} \quad \ddot{\beta}\,]^T$, i.e.: $\boldsymbol{z}_{lat}^{(r)} = A_x\boldsymbol{x}_{lat} + B_u\overline{\boldsymbol{u}}_{lat} + G'_{lat}\tilde{\boldsymbol{u}}_{lat}$, where $\overline{\boldsymbol{u}}_{lat} = [\,\overline{\delta}_{a_c} \quad \overline{\delta}_{r_c}\,]^T$, $\tilde{\boldsymbol{u}}_{lat} = \begin{bmatrix} V_{vy} & \widetilde{V}_{vy} \end{bmatrix}^T$, $A_x = \begin{bmatrix} a'_{61} & a'_{62} & a'_{63} & a'_{64} & 0 & 0 & a'_{67} & a'_{68} \\ a'_{11} & a'_{12} & a'_{13} & a'_{14} & 0 & 0 & a'_{17} & a'_{18} \end{bmatrix}$, $B_u = \begin{bmatrix} -\frac{V_0 b_{11}}{T_a} & -\frac{V_0 b_{12}}{T_r} \\ \frac{b_{11}}{T_a} & \frac{b_{12}}{T_r} \end{bmatrix}$, $G'_{lat} = \begin{bmatrix} a'_{31} & -a_{11} \\ -\frac{a'_{11}}{V_0} & \frac{a_{11}}{V_0} \end{bmatrix}$. The form of the control law $\bar{\boldsymbol{u}}_{lat}$ results from $\boldsymbol{z}_{lat}^{(r)} = A_x\boldsymbol{x}_{lat} + B_u\overline{\boldsymbol{u}}_{lat} + G'_{lat}\tilde{\boldsymbol{u}}_{lat}$, if one imposes the convergence of $z_{lat}^{(r)} = [\,\dddot{Y} \quad \ddot{\beta}\,]^T$ to $\overline{z}_{lat}^{(r)} = [\,\overline{\dddot{Y}}\,\overline{\ddot{\beta}}\,]^T$ and the convergence of the system estimated state $(\widehat{\boldsymbol{x}}_{lat})$ to $\boldsymbol{x}_{lat}$; in these conditions, one gets [1]:

$$\overline{\boldsymbol{u}}_{lat} = B_u^{-1}\left(\overline{\boldsymbol{z}}_{lat}^{(r)} - A_x\widehat{\boldsymbol{x}}_{lat} - G'_{lat}\tilde{\boldsymbol{u}}_{lat}\right). \tag{16}$$

3.4. Design of the control law's second component (lateral-directional plane)

To obtain the second component of the command law $\boldsymbol{u}_{lat}$, the H-inf control is used; the state equation associated to aircraft dynamics in lateral-directional plane, the equations associated to $z_1 = Y$ and $z_2 = \beta$, as well as the equation of the output vector $\boldsymbol{y}_{lat}$, may be combined into the following equation:

$$\begin{bmatrix} \dot{\boldsymbol{x}}_{lat} \\ z_1 \\ z_2 \\ \boldsymbol{y}_{lat} \end{bmatrix} = \begin{bmatrix} A_{lat} & B_{lat} & G_{lat} & 0_{(8\times 7)} \\ C_{0lat} & D_{01lat} & 0_{(1\times 1)} & 0_{(1\times 7)} \\ C_{1lat} & D_{11lat} & 0_{(1\times 1)} & 0_{(1\times 7)} \\ C_{lat} & 0_{(7\times 2)} & 0_{(7\times 1)} & D_{22lat} \end{bmatrix} \begin{bmatrix} \boldsymbol{x}_{lat} \\ \boldsymbol{u}_{lat} \\ \tilde{\boldsymbol{u}}_{lat} \\ \boldsymbol{e}_{lat} \end{bmatrix}; \tag{17}$$

the matrices $A_{lat}, B_{lat}, G_{lat}$ have the forms (13) and $C_{0lat} = [\,0\ 0\ 0\ 0\ 0\ 1\ 0\ 0\,]$, $C_{1lat} = [\,1\ 0\ 0\ 0\ 0\ 0\ 0\ 0\,]$, $D_{01lat} = [\,c_1 \quad 0\,]$, $D_{11lat} = [\,0 \quad c_2\,]$; the matrix D_{22lat} has the form $D_{22\ lat} = I_7$ for the vector containing the sensor errors: $\boldsymbol{e}_{lat} = \begin{bmatrix} e_Y & e\dot{Y} & e_\beta & e_\phi & e_p & e_\psi & e_r \end{bmatrix}^T$. It is known that the sensors (used to measure some important variables) have sometimes errors; for example, the most important errors of a gyro sensor are [1]: 1) the bias; 2) the scale factor; 3) the calibration error of the scale factor; 4) the

noise of the sensor; 5) the sensibility to an acceleration applied along an arbitrary direction. The bias and the noise are the most severe for the control performance during landing. Usually, on aircraft, there are used gyros to measure the angular rates (e.g. p and r); by integration of these angular rates, one obtains the roll and yaw angles. Because on aircraft there are also transducers (sensors) for the attack angle and for the sideslip angle (β), in this chapter, one considered sensor errors for β, p, and r. Similar remarks can be done for the automatic landing subsystem in longitudinal plane. In the software validation of the two automatic landing subsystems, the authors will use some information from [1], but the values of the sensors' errors will be increased to analyze the robustness of the two ALS subsystems. Also, it is interesting to proof that, for the steady regime, the forms of $z_1 = Y$ and $z_2 = \beta$ are the same with the expressions in (17); the expansion of $\boldsymbol{z}_{lat} = [\,z_1 \quad z_2\,]^T$ as function of state ($\boldsymbol{x}_{lat}$) and of the system command vector ($\boldsymbol{u}_{lat}$) leads to the equations:

$$\boldsymbol{z}_{lat} = \begin{bmatrix} z_1 \\ z_2 \end{bmatrix} = \boldsymbol{z}_{lat}\,(\boldsymbol{x}_{lat},\ \boldsymbol{u}_{lat}) \cong \underbrace{\boldsymbol{z}_{lat}\,(\boldsymbol{x}_{lat\,0},\ \boldsymbol{u}_{lat\,0})}_{z_{lat_0}} + \left(\frac{\partial \boldsymbol{z}_{lat}}{\partial \boldsymbol{x}_{lat}}\right)_{(x_{lat\,0},\ 0)} \Delta x_{lat} + \left(\frac{\partial \boldsymbol{z}_{lat}}{\partial \boldsymbol{u}_{lat}}\right)_{\left(\boldsymbol{x}_{lat_0},\ 0\right)} \Delta \boldsymbol{u}_{lat} \cong \boldsymbol{z}_{lat_0}$$

$$+ \underbrace{\begin{bmatrix} \frac{\partial z_1}{\partial x_1} & \cdots & \frac{\partial z_1}{\partial x_n} \\ \frac{\partial z_2}{\partial x_1} & \cdots & \frac{\partial z_2}{\partial x_n} \end{bmatrix}_{\left(\boldsymbol{x}_{lat_0},0\right)}}_{\begin{bmatrix} C_{0lat} \\ C_{1lat} \end{bmatrix}} \Delta \boldsymbol{x}_{lat} + \underbrace{\begin{bmatrix} \frac{\partial z_1}{\partial u_1} & \frac{\partial z_1}{\partial u_2} \\ \frac{\partial z_2}{\partial u_1} & \frac{\partial z_2}{\partial u_2} \end{bmatrix}_{\left(\boldsymbol{x}_{lat_0},\ 0\right)}}_{\begin{bmatrix} D_{01lat} \\ D_{11lat} \end{bmatrix}} \Delta \boldsymbol{u}_{lat} \Leftrightarrow \Delta \boldsymbol{z}_{lat} \cong \begin{bmatrix} C_{0lat} \\ C_{1lat} \end{bmatrix} \Delta \boldsymbol{x}_{lat}$$

$$+ \begin{bmatrix} D_{01lat} \\ D_{11lat} \end{bmatrix} \Delta \boldsymbol{u}_{lat} \Leftrightarrow \boldsymbol{z}_{lat} \cong \begin{bmatrix} C_{0lat} \\ C_{1lat} \end{bmatrix} \boldsymbol{x}_{lat} + \begin{bmatrix} D_{01lat} \\ D_{11lat} \end{bmatrix} \boldsymbol{u}_{lat} \cong \overline{C}_{lat} \boldsymbol{x}_{lat} + \overline{D}_{lat} \boldsymbol{u}_{lat}, \quad \text{with}$$

$C_{0lat} = \begin{bmatrix} \frac{\partial z_1}{\partial x_1} & \cdots & \frac{\partial z_1}{\partial x_n} \end{bmatrix}_{\left(\boldsymbol{x}_{lat_0},\ 0\right)}$, $C_{1lat} = \begin{bmatrix} \frac{\partial z_2}{\partial x_1} & \cdots & \frac{\partial z_2}{\partial x_n} \end{bmatrix}_{\left(\boldsymbol{x}_{lat_0},\ 0\right)}$; $x_i\left(i = \overline{1,\ n}\right)$ are the system's states (n = 8), $D_{01lat} = \left[\frac{\partial Y}{\partial \delta_{ac}} \frac{\partial Y}{\partial \delta_{rc}}\right]_{\left(\boldsymbol{x}_{lat_0},0\right)} = [c_1\, 0], D_{11lat} = \left[\frac{\partial z_2}{\partial u_1} \frac{\partial z_2}{\partial u_2}\right]_{\left(\boldsymbol{x}_{lat_0},0\right)} = \left[\frac{\partial \beta}{\partial \delta_{ac}} \frac{\partial \beta}{\partial \delta_{rc}}\right]_{\left(\boldsymbol{x}_{lat_0},0\right)} = [0\, c_2], \overline{C}_{lat} = \begin{bmatrix} C_{0lat} \\ C_{1lat} \end{bmatrix}$, $\overline{D}_{lat} = \begin{bmatrix} D_{01lat} \\ D_{11lat} \end{bmatrix}$. c_1 and c_2 have small positive values; in steady regime ($\boldsymbol{u}_{lat}$ = 0), one gets $z_1 = Y$ and $z_2 = \beta$.

The optimal control law in lateral-directional plane has the form [14]: $\boldsymbol{u}_{\infty lat} = -K_{\infty lat}(\widehat{\boldsymbol{x}}_{lat} - \overline{\boldsymbol{x}}_{lat})$, $K_{\infty lat} = R_1^{-1} B_{lat}{}^T P_\infty$, $R_1 = \overline{D}_{lat}{}^T \overline{D}_{lat}$; $\boldsymbol{u}_{\infty\ lat}$ must minimize the cost functional $J_{lat} = \frac{1}{2}\int_0^\infty \boldsymbol{z}_{lat}{}^T \boldsymbol{z}_{lat} \mathrm{d}t =$

$= \frac{1}{2}\int_0^\infty \left[\boldsymbol{x}_{lat}^T \underbrace{(\overline{C}_{lat}^T \overline{C}_{lat})}_{Q_1} \boldsymbol{x}_{lat} + \boldsymbol{u}_{\infty\ lat}^T \underbrace{(\overline{D}^T \overline{D})}_{R_1} \boldsymbol{u}_{\infty lat}\right] \mathrm{d}t$. The symmetric and positive defined matrix P_∞ is the stabilizing solution of the Riccati matriceal equation [1]:

$$A_{lat}^T P_\infty + P_\infty A_{lat} - P_\infty \left(B_{lat} R_1^{-1} B_{lat}^T - \mu_1^{-2} G_{lat} G_{lat}^T\right) P_\infty + Q_1 = 0. \tag{18}$$

The remarks regarding Q_1, R_1, and μ_1 remain the same; the controller gain matrix ($K_{\infty lat}$) has the general form $K_{\infty lat} = R_1^{-1} B_{lat}^T P_\infty$ which is typical for the optimal control theory. The optimal

control law $\boldsymbol{u}_{\infty lat}$ depends on $\Delta\widehat{\boldsymbol{x}}_{lat} = \widehat{\boldsymbol{x}}_{lat} - \overline{\boldsymbol{x}}_{lat}$, as one can see above. To obtain this signal, the observer presented above is again used; this time, one obtains the estimated state vector $(\widehat{\boldsymbol{x}}_{lat})$ and the signal $\Delta\widehat{\boldsymbol{x}}_{lat} = \widehat{\boldsymbol{x}}_{lat} - \overline{\boldsymbol{x}}_{lat}$; the equation of the observer is

$$\Delta\dot{\widehat{\boldsymbol{x}}}_{lat} = A_{lat}\Delta\widehat{\boldsymbol{x}}_{lat} + B_{lat}\boldsymbol{u}_{lat} + G_{lat}\tilde{\boldsymbol{u}}_{lat} + L_{\infty lat}\left(\Delta y_{lat} - C_{lat}\Delta\widehat{\boldsymbol{x}}_{lat}\right). \tag{19}$$

The observer gain matrix $L_{\infty lat}$ is calculated by using the formula: $L_{\infty lat} = P_{\infty}^{*}C_{lat}^{T}\left(D_{22lat}^{T}D_{22lat}\right)^{-1}$, with P_{∞}^{*}– the stabilizing solution of the Riccati matriceal equation [15]:

$$A_{lat}P_{\infty}^{*} + P_{\infty}^{*}A_{lat}^{T} - P_{\infty}^{*}\left(C_{lat}^{T}C_{lat} - \mu_2^{-2}\overline{C}_{lat}^{T}\overline{C}_{lat}\right)P_{\infty}^{*} + G_{lat}G_{lat}^{T} = 0; \tag{20}$$

μ_2 is a small positive scalar for which the Riccati equation (20) has a stabilizing solution; one used the same notations for the matrices Q_1, R_1, P_{∞}, and P_{∞}^{*} but their values are completely different from the ones in the case of aircraft motion in longitudinal plane.

4. Structure of the complete automatic landing system

To control all the variables in longitudinal plane, one also uses two reference models (**Figure 1a**) providing the desired altitude, velocity on the landing curve, and their derivatives up to relative degrees of the system [16]. Aircraft desired state $\left(\overline{\boldsymbol{x}}_{long}\right)$ and the desired output vector $\left(\overline{\boldsymbol{y}}_{long}\right)$ are obtained by using the states of the reference models. The optimal control is calculated on-line by means of the error $\Delta\boldsymbol{x}_{long} = \hat{\boldsymbol{x}}_{long} - \overline{\boldsymbol{x}}_{long}$.

4.1. Block diagrams of the reference models

The two reference models (the former being a three order reference model, while the latter is a second order reference model) are also used for the calculation of the vector $\overline{\boldsymbol{Z}}$. The two reference models receive information from a block which models the geometry of landing in longitudinal plane; this block uses two equations—one for the glide slope phase and one for the flare phase. The equation associated to the glide slope phase ($H \geq \overline{H}_0$, $\overline{H}_0$– the altitude at which the glide slope phase ends and the second landing phase begins) is [10]:

$$\overline{H} = \left(X - X_{p_0}\right)\tan\left(\gamma_c\right), \tag{21}$$

where X is the covered distance, horizontally measured, X_{p_0}– describes the point where the horizontal axis intersects the glide slope, $\overline{H}$– the desired altitude, while γ_c is the aircraft desired slope angle. The seven components of the imposed vector $\overline{\boldsymbol{Z}}$ are: $\overline{H}$, $\dot{\overline{H}} = u \cdot \gamma_c$, $\ddot{\overline{H}} = 0$, $\dddot{\overline{H}} = 0$, $\overline{u} = u_0 \cong V_0$, $\dot{\overline{u}} = 0$, and $\ddot{\overline{u}} = 0$. The equation associated to the flare phase $\left(H < \overline{H}_0\right)$ is [10]:

$$\overline{H} = \overline{H}_0 \exp(-t/\tau), \tag{22}$$

with τ − the time constant that defines the exponential curvature (the flare phase); as a consequence, $\dot{\overline{H}} = -\frac{1}{\tau}\overline{H}$, $\ddot{\overline{H}} = \frac{1}{\tau^2}\overline{H}$, $\dddot{\overline{H}} = -\frac{1}{\tau^3}\overline{H}$, $\overline{u} = u_0 \cong V_0$, $\dot{\overline{u}} = 0$, $\ddot{\overline{u}} = 0$ .. If the reference models in **Figure 1a** are used, the roles of the variables $\overline{H}$ and $\bar{u}$ from (21) and (22) are played by the variables H_c and u_c, respectively; the variables $\dddot{\overline{H}}$, $\ddot{\overline{H}}$, $\dot{\overline{H}}$, $\overline{H}$, $\ddot{\overline{u}}$, $\dot{\overline{u}}$, and $\bar{u}$ are provided by the reference models.

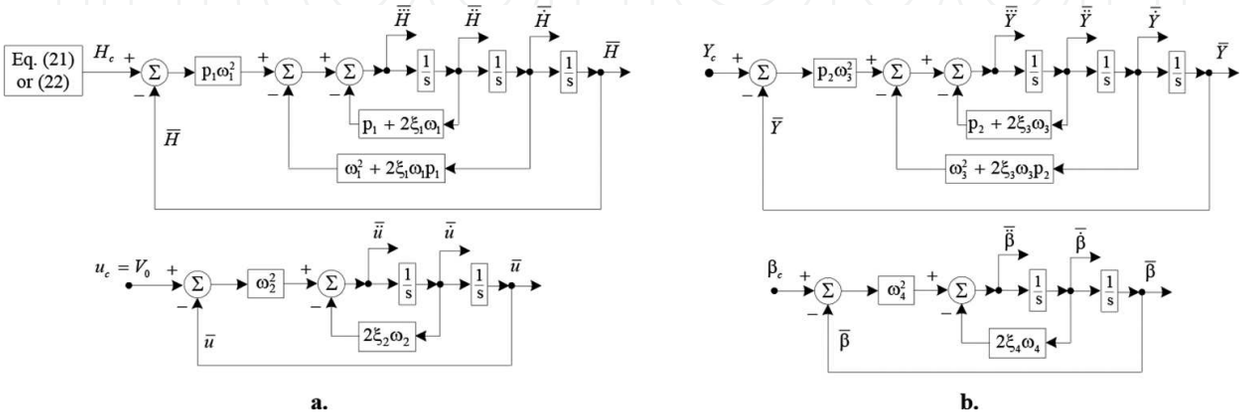

Figure 1. Block diagrams of the reference models.

Similar approach is used for aircraft motion in lateral-directional plane; the vectors $\overline{z}$ and $z_{lat}^{(r)}$ are calculated by means of other two reference models, the former being a three-order reference model (associated to Y), while the latter is a second-order reference model (associated to β) (**Figure 1b**) [1].

4.2. The block diagram of the new automatic landing system

The structure of the new ALS, using dynamic inversion and H-inf method, is presented in **Figure 2**; it consists of two subsystems—the first one controls aircraft motion in longitudinal plane, while the second one is for the control of aircraft motion in lateral-directional plane.

In longitudinal plane, to track the desired trajectory, one must control the aircraft speed (u) and its altitude (H). The landing requirements involve the aircraft descend to an altitude of 420 m above the ground in the same time with the reduction of its speed from the cruise value to the landing value (70 m/s); then, the speed should be maintained constant. In lateral-directional plane, the desired landing trajectory of aircraft mainly involves two variables' control: the aircraft lateral deviation with respect to the runway (Y) and the sideslip angle (β).

In longitudinal plane, the dynamic inversion and H-inf method must assure the convergences:
$\Delta \boldsymbol{y}_{long} \to 0\left(\boldsymbol{y}_{long} = C_{long}\boldsymbol{x}_{long} \to \overline{\boldsymbol{y}}_{long} = C_{long}\overline{\boldsymbol{x}}_{long}, \boldsymbol{x}_{long} \to \overline{\boldsymbol{x}}_{long}\right)$
$\Delta \boldsymbol{z}_{long} \to 0\left(\boldsymbol{z} = C'_{long}\boldsymbol{x} \to \overline{\boldsymbol{z}} = C'_{long}\overline{\boldsymbol{x}}\right),\ \Delta\widehat{\boldsymbol{x}}_{long} \to 0\left(\widehat{\boldsymbol{x}}_{long} \to \boldsymbol{x}_{long} \to \overline{\boldsymbol{x}}_{long}\right),$
$\boldsymbol{u}_{\infty long} \to 0,\ \overline{\boldsymbol{u}}_{long} \to 0,\ \boldsymbol{u}_{long} \to 0$; in lateral-directional plane, the following convergences should

http://dx.doi.org/10.5772/62666

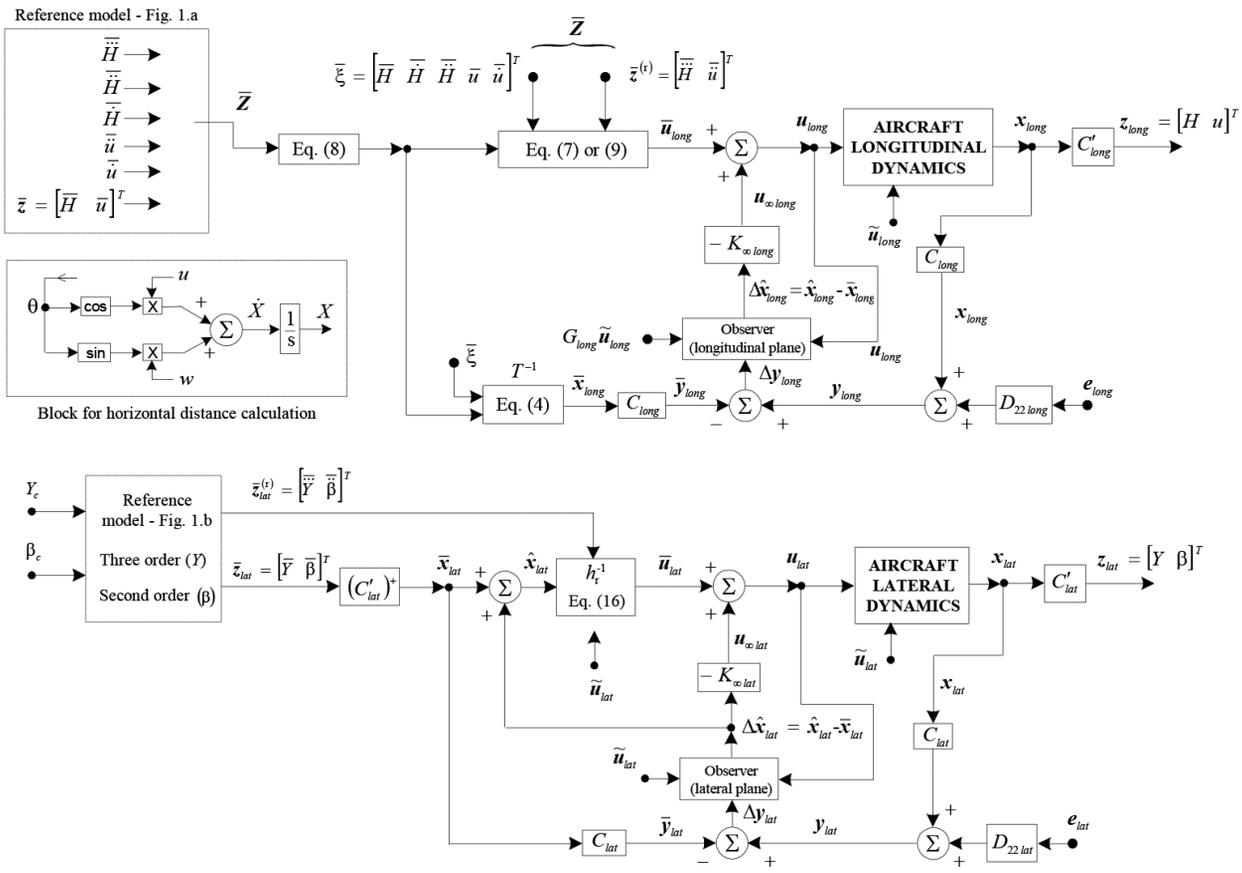

Figure 2. Structure of the new architecture for aircraft automatic control during landing.

be assured: $\Delta \boldsymbol{y}_{lat} \to 0 \left(\boldsymbol{y}_{lat} = C_{lat} \boldsymbol{x}_{lat} \to \overline{\boldsymbol{y}}_{lat} = C_{lat} \overline{\boldsymbol{x}}_{lat},\ \boldsymbol{x}_{lat} \to \overline{\boldsymbol{x}}_{lat} \right),\ \Delta z_{lat} \to 0$ $\left(\boldsymbol{z} = C'_{lat} \boldsymbol{x} \to \overline{\boldsymbol{z}} = C'_{lat} \overline{\boldsymbol{x}} \right),\ \Delta \widehat{\boldsymbol{x}}_{lat} \to 0 (\widehat{\boldsymbol{x}}_{lat} \to \boldsymbol{x}_{lat} \to \overline{\boldsymbol{x}}_{lat}),\ \boldsymbol{u}_{\infty lat} \to 0,\ \overline{\boldsymbol{u}}_{lat} \to 0,\ \boldsymbol{u}_{lat} \to 0.$

5. Numerical simulation results

5.1. Numerical simulation setup

In order to analyze the behaviour and the performances of the designed ALS, one considers a numerical example associated to the flight of a Boeing 747. The Matlab/Simulink environment is used for complex simulations; to obtain the time histories of the main variables describing the aircraft motion in longitudinal and lateral-directional planes, one software implemented the two optimal observers, the four reference models, and the two H-inf controllers.

For aircraft dynamics in lateral-directional plane, the values of the coefficients are [11]: $a_{11} = -0.0013,\ a_{12} = 0,\ a_{13} = -1,\ a_{14} = 0.15,\ a_{21} = -1.33,\ a_{22} = -0.98,\ a_{23} = 0.33,\ a_{31} = 0.17,$ $a_{32} = -0.17,\ a_{33} = -0.217,\ b_{11} = 0.001,\ b_{12} = 0.015,\ b_{21} = 0.23,\ b_{22} = 0.06,\ b_{31} = 0.026,\ b_{32} = -0.15,$ $V_0 = 67$ m/s, $T_a = 0.7$ s, $T_r = 0.1$s, $\mu_1 = 1,\ \mu_2 = 1,\ c_1 = c_2 = 0.01,\ \overline{Y} = 0$m, $\overline{\beta} = 0$ deg; the vector of sensor errors has been chosen as: $\boldsymbol{e}_{lat}$ = [0 m 0 m/s 1 deg 0 deg 1 deg/s 0 deg 1 deg/s]^T, the matrix G_{lat} has been obtained by means of the equation (13), while the system's initial state is

$\boldsymbol{x}_{lat}(0) = [0.1\text{deg} \quad 0\text{deg/s} \quad -2\text{deg/s} \quad 0\text{deg} \quad 0.1\text{deg} \quad 25\text{m} \quad 0\text{deg} \quad 0\,\text{deg}]^T$; for the reference models, one has chosen: $p_2 = 25, \xi_3 = \xi_4 = 0.7, \omega_3 = \omega_4 = 2$ rad/s. To test the robustness of the new ALS (lateral-directional plane) with respect to the crosswind (lateral wind—V_{vy}), in simulations different values for $\tilde{\boldsymbol{u}}_{lat} = V_{vy}$ between 2 and 10 m/s are considered. The values considered here for the sensors' errors (both planes—longitudinal and lateral-directional) are chosen very large because it is important to use strong disturbances instead of small ones when designing a robust ALS.

For aircraft dynamics in longitudinal plane, the values of the coefficients for Boeing 747 have been borrowed from [11]: $a_{11} = -0.021$, $a_{12} = 0.122$, $a_{14} = -0.322$, $a_{21} = -0.209$, $a_{22} = -0.53$, $a_{23} = 2.21$, $a_{31} = 0.017$, $a_{32} = -0.164$, $a_{33} = -0.412$, $a_{52} = -1$, $a_{54} = V_0 = 70$ m/s, $b_{11} = 0.01$, $b_{12} = 1$, $b_{21} = -0.064$, $b_{22} = -0.044$, $b_{31} = -0.378$, $b_{32} = 0.544$, $T_e = 0.3$ s, $T_T = 2$ s, $\bar{u} = V_0, V_{vx0} = 1$ m/s, $V_{vz0} = 1$ m/s $T_0 = 30$ s. The vector of sensor errors is $\boldsymbol{e}_{long} = [0.2$ m 0.2 deg/s 0.2 m 0 m/s^2 0.2 deg 0.1 deg/s$]^T$, while, for the reference models, one has chosen: $p_1 = 25, \xi_1 = \xi_2 = 0.7$, $\omega_1 = \omega_2 = 2$ rad/s. For the first landing phase in longitudinal plane, the following values have been used: $\overline{H}_p = \overline{H}(0) = 420\text{m}, X(0) = 0, X_{p_0} = -\overline{H}_p/\tan(\gamma_c), \gamma_c = -2.5$ deg. The other components of vector $\overline{\xi}$ are provided by the reference models, $\eta(0) = [-4.2$ deg -0.46 deg/s$]^T$, $\mu_1 = 50$, $\mu_2 = 1$, while the initial value of the state is $\boldsymbol{x}_{long}(0) = [72$ m/s $\quad -3.1$ m/s $\quad 0$ grd/s -0.6 deg $\quad 420$ m $\quad 0$ deg $\quad 0$ deg$]^T$.

5.2. Results and discussion

In **Figure 3**, one represents the time characteristics for the flight direction control system (the second subsystem of the complete ALS in **Figure 2**); before the start of the two landing main stages in longitudinal plane, the pilot must cancel aircraft's lateral deviation with respect to the runway. The characteristics have been represented for the first ALS affected by crosswind (V_{vy} = 2 m/s) in the presence or in the absence of sensor errors (the sensors are used for the measurement of the states). The presence of the sensor errors is not visible—the curves with solid line (obtained in the absence of sensor errors) overlap almost perfectly over the curves plotted with dashed line (obtained in the presence of sensor errors).

The landing approach (the only landing phase which takes place in the lateral-directional plane) begins at the nominal speed of 67 m/s; the speed should be maintained constant. To test the robustness of the first designed ALS, in the simulations for lateral-directional plane, one has taken into consideration the crosswind, because low-altitude crosswind can be a serious threat to the safety of aircraft in landing. From sixth mini-graphic in **Figure 3** (achieved for V_{vy} = 2 m/s), one can see that the stationary value of Y (aircraft lateral deviation) is very close to zero; analyzing the Aviation Administration (FAA) accuracy requirements for Category III (best category) [17], one can remark that this error is very good; for best category, it must less than 4.1 m, for Category II precision standards, the error must be between 4.1 and 4.6 m, while Category I precision standards involve an error between 4.6 and 9.1 m. The H-inf control technique is ideal for handling plants affected by sensor errors, measurement noise, or other disturbances (e.g. crosswind). Because the convergence error of the sideslip angle is less than 0.01 deg, one can notice the convergence $\beta \to \beta_c = 0$ deg.

http://dx.doi.org/10.5772/62666

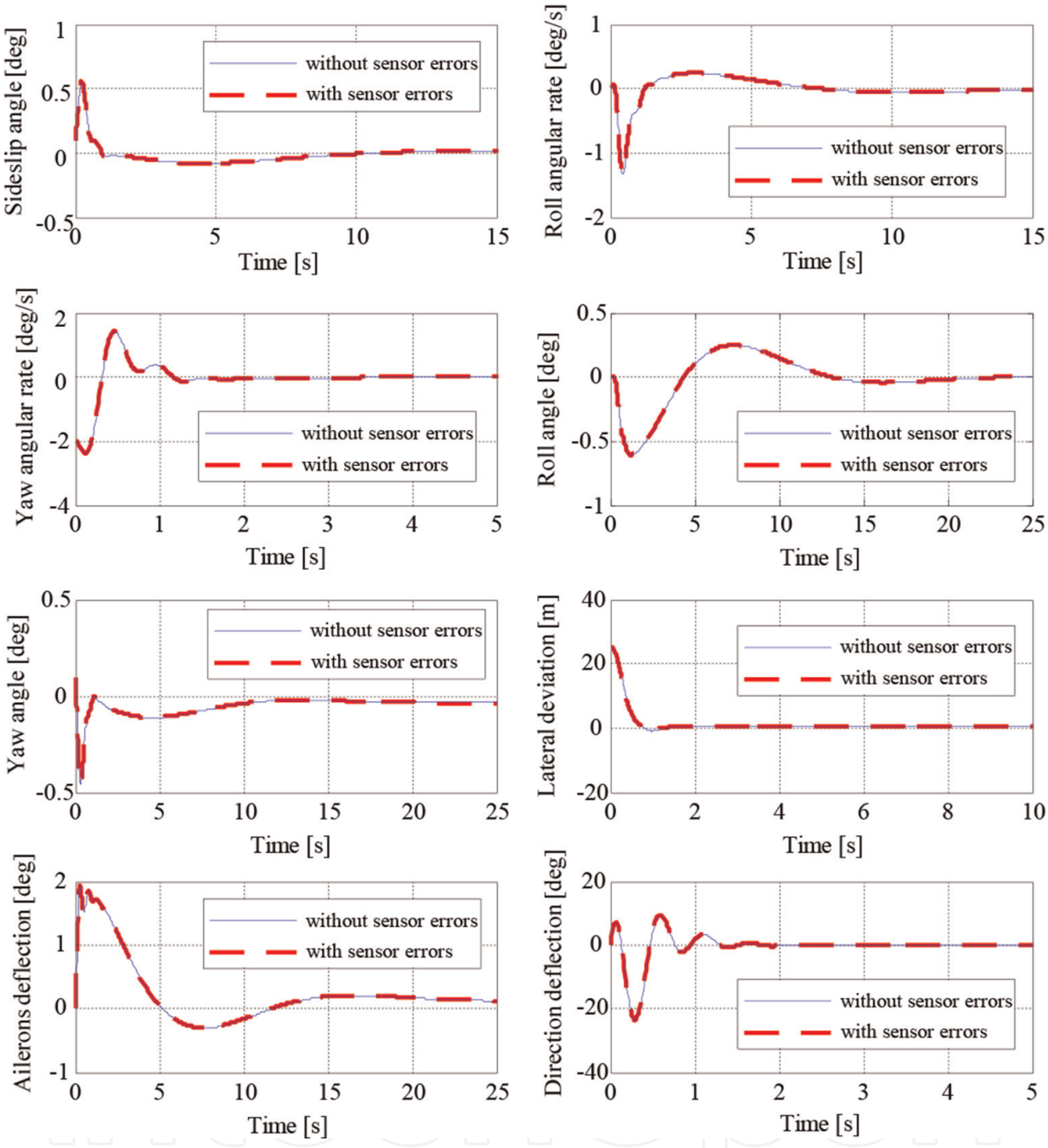

Figure 3. Time characteristics of the lateral-directional control subsystem.

In **Figures 4** and **5**, there are represented the time characteristics for the glide slope landing phase and flare landing phase, respectively; the characteristics have been represented for the ALS affected by wind shears in the presence or in the absence of sensor errors. The last four mini-graphics in **Figures 4** and **5** represent the differences between the real values of the speed (u), sink rate ($.H$), slope angle (γ), altitude (H) and the desired values of these variables: $u-\overline{u}$, $.H-\overline{.H}$, $\gamma-\gamma_c$, $H-\overline{H}$. As in the case of aircraft motion in lateral-directional plane, the sensor errors do not affect the landing. One may also remark in **Figures 4** and **5** that the slope

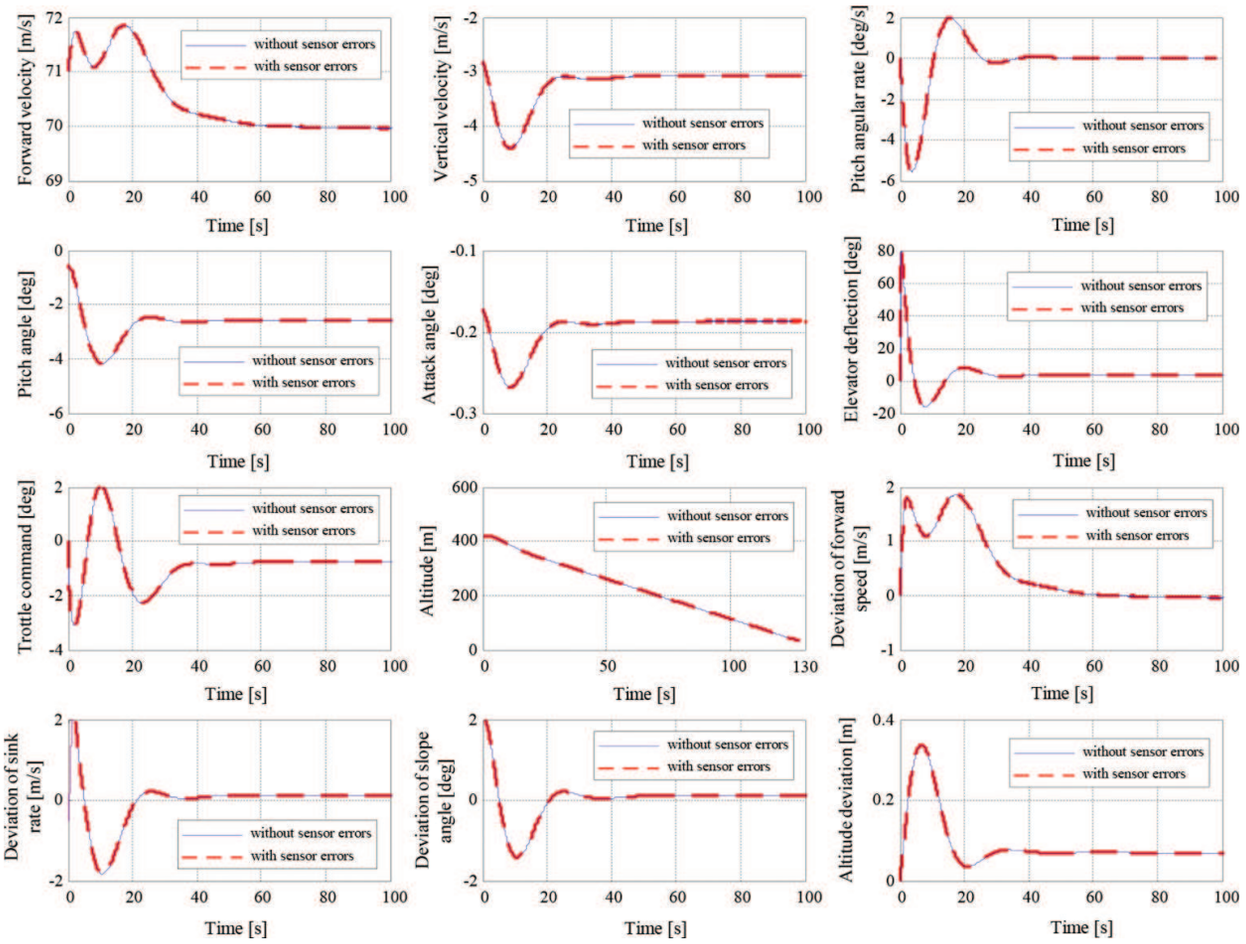

Figure 4. Time characteristics of ALS, for the glide slope phase, with or without sensor errors.

angle is in perfect accord with its desired values: −2.5 degrees during glide slope phase and 0 degrees during flare, respectively. During the glide slope phase, the aircraft describes a linear descendent trajectory (eighth graphic in **Figure 4**), while in the flare phase, it describes a parabolic trajectory (eighth graphic in **Figure 5**) with a null slope angle.

In longitudinal plane, to test the robustness of the new ALS, in all simulations, one has taken into consideration the wind shears. **Figures 4** and **5** prove that the altitude error (the difference between the desired path and the actual path) is less than 0.3 m during the first landing stage (longitudinal plane) and less than 0.2 m during the second landing stage (longitudinal plane). According to the Federal Aviation Administration (FAA) accuracy requirements for Category III [17], the resulted errors are very small; thus, according to FAA Category III accuracy requirements, the vertical error (altitude deviation with respect to its nominal value) must be less than 0.5 m, while the final altitude at the end of flare must be 0 m. The ALS designed in this chapter meets the requirement because the H-inf robust control technique has been used; this method can handle the plant with measurement noise (sensor errors) and wind shears.

5.3. Comparison with other works

The ALS designed in this chapter represents an improved version of the ALS designed in [11] and it differs from other similar ALSs from the specialty literature; first of all, our ALS is not

http://dx.doi.org/10.5772/62666

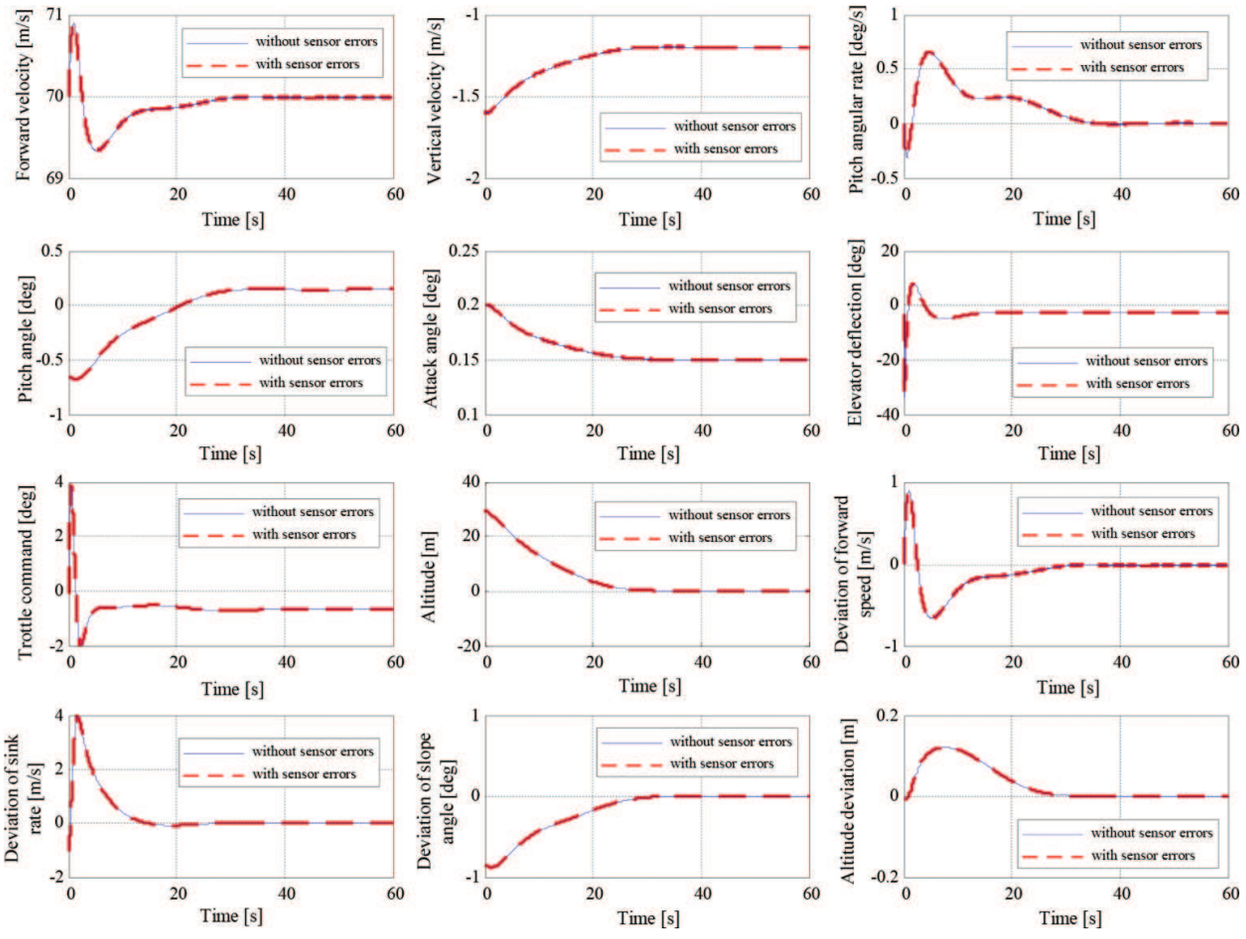

Figure 5. Time characteristics of ALS, for the flare phase, with or without sensor errors.

designed only for the longitudinal (vertical) plane but also for the lateral-directional plane; two subsystems have resulted, the new ALS being the mixture of these two automatic landing subsystems. Our new ALS has some additional elements with respect to the one presented in [11]: two optimal observers and four reference models which provide the desired altitude, velocity on the landing curve, their derivatives up to relative degrees of the system, the desired lateral deviation with respect to the runway, and the desired sideslip angle.

The results in this work have been compared to the ones obtained in [2] where the authors have designed a system which controls the lateral angular deviation of aircraft longitudinal axis with respect to the runway, by using a classical controller, a radio-navigation system, a system for the calculation of the distances between aircraft and the runway radio-markers, and an adaptive controller mainly used for the control of aircraft roll angle and its deviation with respect to the runway; the adaptive control system uses the dynamic inversion concept, a dynamic compensator, a neural network trained by the system's estimated error vector (signal provided by a linear observer), and a Pseudo Control Hedging block. The time regime period is better in our work (almost 15 seconds) but the lateral deviation's overshoot is larger; therefore, one can conclude that the neural networks-based adaptive controllers are more efficient than the conventional ones for aircraft landing in lateral-directional plane but their main disadvantage is that the neural networks require a priori training on normal and faulty operating data and these are enable only under limited conditions; on the other hand, the

usage of Pseudo Control Hedging blocks (when the actuators are nonlinear) does not modify the final values of the variables. For the same aircraft type, same direction controller, and radio-navigation system but with a proportional-derivative type control after the roll angle and a proportional type control after $\Delta\psi$ [18], there have been obtained performance inferior to those obtained here by using the H-inf control, the dynamic inversion, optimal observers, and reference models.

The problem of landing in longitudinal plane has been also discussed in other papers, different types of ALSs being designed [9, 10]. If one makes a brief comparison between our ALS (longitudinal plane) and the ones based on an Instrumental Landing System or conventional/fuzzy control of flight altitude by using the system's state [9], one remarks that from the system transient regime period and overshoot's points of view, the ALS based on the H-inf technique and dynamic inversion works slightly better. Improvement of the performance was obtained by replacing the conventional controllers with fuzzy controllers [9], but those ALSs cannot be used for no-bounded exogenous signals or strongly nonlinear aircraft dynamics. Our new ALS uses the H-inf technique, this having the advantage over classical control techniques in that it has applicability to problems involving multivariate systems with cross-coupling between channels; the only disadvantage is related to the non-linear constraints which are generally not well-handled.

5.4. Current and future work

This chapter presents some of the work that has been carried out at Laboratory of Aerospace Engineering, University of Craiova. Till now, there have been designed and software implemented: 1) two new ALSs (longitudinal plane) using the Instrumental Landing System and the flight altitude's control by means of the state vector (the controllers of the ALSs are designed both with classical and fuzzy logic approaches); 2) a new ALS (longitudinal plane) using the dynamic inversion concept and PID controllers in conventional and fuzzy variants, taking into consideration the wind shears and sensor errors; 3) a new ALS (lateral-directional plane) which controls the lateral angular deviation of aircraft longitudinal axis with respect to the runway, by using a classical controller, a radio-navigation system, a system for the calculation of the distances between aircraft and the runway radio-markers, and an adaptive controller mainly used for the control of aircraft roll angle and its deviation with respect to the runway. Our future work will focus on the design of ALSs (mixtures between subsystems designed for the longitudinal and lateral-directional planes) putting together the dynamic inversion technique, dynamics compensators, feed-forward neural networks, and Pseudo Control Hedging blocks.

6. Conclusions

The purpose of this study was to design a robust ALS by using the H-inf and dynamic inversion techniques taking into consideration the sensor errors and other different disturbances; two landing subsystems have been designed, software implemented and validated; the first subsystem is useful for landing control in longitudinal plane, while the second one is

used in lateral-directional plane. After the separate design of the two subsystems, these have been combined to obtain a complete landing auto-pilot. The H-inf control technique handles the plant with measurement noise (sensor errors) and wind shears; the use of the dynamic inversion makes our control system more general and, therefore, it can be used both for the case when aircraft dynamics is nonlinear and for the case when the aircraft dynamics is linear; thus, this technique increases the generality character of our new ALS. Promising results have been obtained; these prove the robustness of the designed ALS even in the presence of disturbances and sensor errors.

Acknowledgements

This work is supported by the grant no. 89/1.10.2015 of the Romanian National Authority for Scientific Research and Innovation, CNCS – UEFISCDI, project code PN-II-RU-TE-2014-4-0849.

Author details

Romulus Lungu* and Mihai Lungu

*Address all correspondence to: romulus_lungu@yahoo.com

University of Craiova, Faculty of Electrical Engineering, Craiova, Romania

References

[1] Lungu R, Lungu M. Automatic control of aircraft in lateral-directional plane during landing. Asian Journal of Control. 2016; 18: 1–16.

[2] Lungu M, Lungu R. Automatic control of aircraft lateral-directional motion during landing using neural networks and radio-technical subsystems. Neurocomputing Journal. 2016; 171: 471–481.

[3] Singh S, Padhi R. Automatic path planning and control design for autonomous landing of UAVs using dynamic inversion. American Control Conference Riverfront, St. Louis, MO, 2009; p. 2409–2414.

[4] Wagner T, Valasek J. Digital autoland control laws using quantitative feedback theory and direct digital design. Journal of Guidance, Control, and Dynamics. 2007; 30: 1399–1413.

[5] Kumar V, Rana KP, Gupt V. Real-time performance evaluation of a fuzzy PI + fuzzy PD controller for liquid-level process. International Journal of Intelligent Control and Systems. 2008; 13: 89–96.

[6] Lau K, Lopez R, Onate E. Neural networks for optimal control of aircraft landing systems. Proceedings of the World Congress on Engineering. 2007; II: 904–911.

[7] Zhi L, Yong W. Intelligent landing of unmanned aerial vehicle using hierarchical fuzzy control. IEEE Aerospace Conference, 2012; p. 1–12.

[8] Ismail S, Pashilkar A, Ayyagari R, Sundararajan N. Improved autolanding controller for aircraft encountering unknown actuator failures. IEEE Symposium on Computational Intelligence for Security and Defense Applications (CISDA), 2013; p. 96–103.

[9] Lungu R, Lungu M, Grigorie TL. Automatic control of aircraft in longitudinal plane during landing. IEEE Transactions on Aerospace & Electronic Systems. 2013; 49: 1338–1350.

[10] Lungu R, Lungu M. Automatic landing control using H-inf control and dynamic inversion. Proceedings of the Institution of Mechanical Engineers Part G – Journal of Aerospace Engineering. 2014; 228: 2612–2626.

[11] Che J, Chen D. Automatic landing control using H-inf control and stable inversion. Proceedings of the 40th Conference on Decision and Control, Orlando, FL, 2001; p. 241–246.

[12] Yu GR. Nonlinear fly-by-throttle H-inf control using neural networks. Asian Journal of Control. 2001; 3: 163–169.

[13] Ochi Y, Kanai K. Automatic approach and landing for propulsion controlled aircraft by H_∞ control. IEEE International Conference on Control Applications, Hawaii, 1999; p. 997–1002.

[14] Stoica AM. Disturbance attenuation and its applications. Romanian Academy Publisher, Bucharest, 2004.

[15] Shue S, Agarwal RK. Design of automatic landing systems using mixed H_2/H_∞ control. Journal of Guidance, Control, and Dynamics. 1999; 22: 103–114.

[16] Lungu M. Sisteme de conducere a zborului [Flight control systems]. Sitech Publisher, Craiova 2008.

[17] Braff R, Powell JD, Dorfler J. Applications of GPS to air traffic control. Global Positioning System: Theory and Applications. 1996; II: 327–374.

[18] Lungu M, Lungu R, Grigorie L. Automatic command systems for the flight direction control during the landing process. Proceedings of International Symposium on Logistics and Industrial Informatics, Budapest, 25–27August 2011; p. 117–122.